

Upper limit magnitudes for induced seismicity in energy industries

Ngoc-Tuyen Cao¹ | Leo Eisner¹  | Zuzana Jechumtálová¹  | James Verdon²  |
 Umair Bin Waheed³ 

¹Seismik s.r.o., Prague, Czech Republic

²School of Earth Sciences, University of Bristol, Bristol, UK

³College of Petroleum Engineering and Geosciences, King Fahd University of Petroleum and Minerals, Dhahran, Saudi Arabia

Correspondence

Zuzana Jechumtálová, Seismik s.r.o., Kubišova 8, 182 00 Prague 8, Czech Republic.

Email: zuzana@seismik.cz

Present addresses

Ngoc-Tuyen Cao, Magnitude, Baker Hugues, Sainte-Tulle, France.

Funding information

College of Petroleum Engineering and Geosciences (CPG); King Fahd University of Petroleum and Minerals (KFUPM), Grant/Award Number: CPG-21103

Abstract

We adopt extreme value theory to estimate the upper limit of the next record-breaking magnitudes of induced seismic events. The methodology is based on order statistics and does not rely on knowledge of the state of the subsurface reservoir or injection strategy. The estimation depends on the history of record-breaking events produced by the anthropogenic activities. We apply the methodology to three different types of industrial operations: natural gas production, saltwater disposal and hydraulic fracturing. We show that the upper limit estimate provides a reliable and realistic upper bound for magnitudes of the record-breaking events in investigated datasets including 15 publicly available datasets. The predicted magnitudes do not overestimate the observed magnitudes by more than 1.0 magnitude unit and underestimation is rare, probably resulting from insufficient sampling of the statistical distribution of the induced seismicity. The richest dataset, sourced from downhole and surface monitoring of the Preston New Road hydraulic fracturing, provides reliable estimates of the magnitudes over three orders of magnitudes with only slight underprediction of the largest observed event. While the detection of weaker events improves the performance of the method, we show that it can be applied even with a few observed record-breaking events to provide reliable estimates of magnitudes. However, care must be taken to ensure that event catalogues are estimated consistently across a range of magnitudes.

KEYWORDS

modeling, passive method, reservoir geophysics, rock physics, seismicity, theory

INTRODUCTION

It is well established that the injection or production of fluids into or from the subsurface can cause induced seismicity (Healy et al., 1968). Injection of fluids can lead to geomechanical destabilization from decreasing effective normal stress with increasing pore pressure (Zoback, 2007). Alternative mechanisms of triggering such as fault reactivation due to cooling (Kivi et al., 2022), compaction (Segall, 1989; Vlek, 2019) or stress changes (Kettlety et al., 2020) have also been identified. The wide range of possible mechanisms that can

cause induced seismicity, combined with the lack of knowledge of the underground stress, temperature and fault structure leads to poor a priori predictability of induced seismicity in space, time and size.

Mitigation of induced seismicity hazard has, therefore, mostly been implemented through the so-called traffic light systems (TLSs; Bommer et al., 2006). TLSs require real-time seismicity monitoring, with mitigating actions implemented as pre-defined magnitude and/or ground motion thresholds are crossed. Specifically, many regulators and operators decide on two thresholds. When the lower threshold ('amber

light') is exceeded, a set of mitigating actions is taken and when the higher threshold ('red light') is exceeded, a more severe action, usually that of suspending the underground operation, is taken. The methodology of setting these thresholds is a topic of current scientific and political discussion (Schultz et al., 2021; Verdon & Bommer, 2021).

TLS thresholds are generally derived from the levels of acceptable, undesirable and unacceptable ground shaking due to induced seismicity. Undesirable levels might be represented by shaking that is above the background seismic noise for the area, where nearby people may sense the earthquake (Mercalli intensity II). Unacceptable levels might be represented by shaking of sufficient energy to cause damage to buildings and infrastructure. However, TLSs are retroactive – actions are taken in response to larger events, rather than in anticipation of them. The occurrence of sharp magnitude 'jumps' (where an event significantly larger than any preceding event occurs) and 'trailing events' (where magnitudes continue to increase after the injection has stopped) mean that an appropriate gap between the red-light threshold and an 'unacceptable' level of shaking must be set to ensure that the latter is not breached (Verdon & Bommer, 2021).

INDUCED SEISMICITY FORECASTING

As an alternative to traffic light systems (TLSs), there is a clear potential to manage induced seismicity through the use of forecasting models. In this approach, models are used to forecast the expected magnitude of upcoming seismicity, with changes in operations being made, if the models indicate that an unacceptable level of seismicity is likely to occur. Even where TLSs are used, operators may wish to make use of such methods to ensure they stay below a red-light threshold at which point they would otherwise be forced to suspend operations.

A range of forecasting methods have been proposed. Some approaches have used numerical geomechanical modelling, either directly simulating fault reactivation (Palgunadi et al., 2020) or as input to hybrid physics-based models where modelled stress changes are used to inform the locations and rates of resulting seismicity (Dahm et al., 2015; Verdon et al., 2015). However, while such simulations clearly have utility in understanding the factors that might promote or inhibit induced seismicity, the use of numerical geomechanical models for induced seismicity forecasting is challenging. The ability to obtain sufficient subsurface information to predict induced seismicity (faults, stress, spatial variations in mechanical properties, etc.) is fundamentally limited by the resolution of geophysical surveying methods (Nantanoi et al., 2022). The lack of understanding of the mechanisms for triggering induced seismicity also limits deterministic prediction. Furthermore, to be operationally useful, seismicity forecasts

may be required in very short timescales (typical hydraulic fracturing and geothermal stimulation operations take place over a period of hours to days), and it can be challenging to generate numerical model results at a usable rate.

A widely applied 'family' of forecasting methods are statistical models where the levels of seismicity are scaled to a metric of industrial activity, such as the injection or production rate (Halló et al., 2014; Mancini et al., 2021; Shapiro et al., 2010; van der Elst et al., 2016). The scaling between the induced seismicity rate and the industrial activity is characterized at an early stage in the process. It is then assumed that this scaling will persist through the operation, and the rates of seismicity are extrapolated to some planned final state (e.g., the total injected volume), from which the final expected earthquake population (and thereby the largest event size) can be estimated. This type of method has been used to manage seismicity during stimulation of the Helsinki geothermal project (Kwiatek et al., 2019) and during hydraulic fracturing of the Preston New Road shale gas wells in Lancashire, UK (Clarke et al., 2019; Kettlety et al., 2021). While this type of approach has shown some predictive capability, there are challenges in their application. For example, in assigning fluid volumes where there may be multiple injection and production wells or in deciding whether it is necessary to agglomerate multiple injection wells and/or stages into a single forecast, or treating each as a separate injection instance (Clarke et al., 2019). These methods may struggle when the initial injection (during which time the model is calibrated) has not reached a large fault, but subsequent reactivation of such a feature produces a sudden change in the levels of seismicity as a function of injection (Kettlety et al., 2021).

An alternative statistics-based approach uses extreme value theory to predict the size of the largest seismic event. This approach is not dependent on subsurface models or knowledge of planned industrial operations (such as injection rates and planned volumes). It has been developed for statistical assessment of maximum values of some observations (Tata, 1969, and later refined by Cooke, 1979, for the prediction of bounds of random variables). The applications of the extreme value theory range from ranking of swimming records (Spearing et al., 2020) to prediction of flooding (Barlow et al., 2020) and include the prediction of largest seismic events, whether natural (Van Aalsburg et al., 2010; Yoder et al., 2010) or induced (Cao et al., 2020; Mendecki, 2012, 2013; Verdon and Bommer, 2021; Varty et al., 2021).

Statistical methods of predicting the largest event do not require a physical understanding of the underlying mechanism of induced seismicity. In fact, these methods are valid for arbitrary mechanisms of induced seismicity and underground distributions of faults, stresses or other parameters but require sufficient sampling of the distribution of the variables before making meaningful predictions. This makes their application to induced seismicity attractive as the monitoring

networks may provide complete sampling of induced seismicity from the start (so long as monitoring networks are installed before the anthropogenic activity begins), and the sampling may start at very weak events if the network is appropriately designed. We note in passing that this is not the case with natural seismicity. A potential drawback of this approach, much like the volume-based methods described above, is the implicit assumption that the distribution of induced seismic events does not significantly change during the anthropogenic operations.

The mining industry has already abandoned the prediction of possible maximum magnitudes using models based on mined volumes as the volumes accounting for seismic and aseismic deformation are not known, and often a seismic monitoring array is installed only once significant seismicity occurs. The current methodologies (Mendecki, 2016) periodically update the maximum possible magnitude associated with extraction as the mining and induced seismicity progresses. Instead, based on observed seismicity, the next record-breaking event (NRBE) and upper limit of the next record-breaking (UL) magnitudes are determined as the most likely and maximum possible magnitudes, respectively.

Cao et al. (2020) applied these estimates to several datasets including the Groningen gas field. Verdon and Bommer (2021) evaluated the performance of the NRBE method using a wide range of hydraulic fracturing-induced seismicity datasets. They found that the NRBE method had an 85% success rate in predicting the next breaking magnitude while avoiding large overprediction, suggesting that the NRBE estimate provides realistic values for maximum magnitude prediction for hydraulic fracturing-induced seismicity. In this study, we have updated the UL and NRBE methodologies to correctly account for maximum magnitudes and show that the UL methodology provides a real upper bound for maximum magnitudes based on observed self-consistent catalogues of seismic events. We emphasize the importance of the catalogue self-consistency, as inaccurate magnitude determination resulting from an inconsistent borehole and surface catalogues does not provide correct estimates.

METHODOLOGY

The methodology proposed by Mendecki (2016) consists of two estimates of the next record-breaking event – its upper limit magnitude (UL) and the most likely magnitude (NRBE). The UL estimate defines the maximum magnitude for a truncated power law distribution of the next seismic event. The UL is estimated only from the previously observed extreme values (in our case previously observed maximum magnitudes). Specifically, the order statistics estimate the next extreme event from the time evolution of the previously observed extremes. The sole requirement of this method

is that the distribution of magnitudes is continuous: this assumption is more general than predictions based on presumed distribution functions (such as the Gutenberg–Richter relationship). Kijko (2004) develop various formulations for maximum magnitudes using extreme value estimators where the Gutenberg–Richter relationship is, or is not, assumed to hold.

In the simplest example, in a dataset where we observe only two record-breaking magnitudes (X_1 and X_2 , $X_1 < X_2$), the order statistics would predict that the UL magnitude would be $X_2 + (X_2 - X_1)$. In other words, we forecast that the next magnitude increase will not exceed the previous magnitude increase. Cooke (1979) shows that for any underlying distribution the estimate of the UL can be made from the previously observed extreme values:

$$M_{UL} = M_{Maxo} + \Delta M_{Max} \quad (1)$$

$$\Delta M_{Max} = 2\Delta M_{Maxo} - \sum_{i=0}^{n-2} \left[\left(1 - \frac{i}{n-1}\right)^{n-1} - \left(1 - \frac{i+1}{n-1}\right)^{n-1} \right] \Delta M_{Maxo - i}, \quad (2)$$

where $\Delta M_{Maxo - i}$ is the ordered differences in magnitude between previous record-breaking events. n is the number of previous record-breaking events. ΔM_{Maxo} is the largest magnitude difference between record-breaking events. This formulation was defined as the NRBE calculation in Cao et al. (2020). We note that Cao et al. (2020) used all observed events ordered by size and the magnitude differences between all events ordered by size as the input to these equations. In this study, we use solely the population of record-breaking events. This is an important difference between Cao et al. (2020) and this study.

The M_{UL} value produced by Equation (1) is the magnitude value which is not expected to be exceeded by the NBRE.

Mendecki (2016) used potency (seismic moment divided by shear modulus) as the variable in Equations (1) and (2) to avoid the sometimes problematic assessment of magnitudes for small events (Kendall et al., 2019). For simplicity, we replace the potency with magnitudes in the following, as magnitude is more widely used, it can be directly linked to other mitigation methods such as traffic light systems (TLSs) and is the normal input for ground motion models used to compute the potential impacts of induced seismicity. It is also a more familiar value for the general public. The derivation assumes that the NBRE is always smaller or equal to the UL value and that the underlying distribution of event values does not change. The assumption of the constant underlying distribution is somewhat problematic for induced seismicity as the human activity driving the seismicity changes (e.g., fracking starts and stops), but Mendecki (2016) shows that this value

gives reasonable estimates in mining settings where involved rock volumes could rapidly change and, therefore, we can assume the distribution is also changing only very slowly in the underground injection/production activities.

It is clear that we need at least two record-breaking events to predict the upper limit and obviously the prediction of the next upper limit magnitude should improve with an increasing number of record-breaking events. Note that Equation (2) puts the most weight on the largest differences. Hence, even if the whole catalogue of events is used, instead of just the record-breaking events, Equation (2) gives very little weight to lower magnitudes in the catalogue. The forecast is, therefore, dependent mainly on the largest magnitudes in the catalogue. In other words, the upper limit estimate primarily relies on previously sampled largest magnitudes to estimate the final upper limit on the magnitude. Analogously, an average swimmer does not help to predict the next record-breaking time in competitive swimming.

Note that the estimator of the upper limit value will improve with the sampling of the distribution, that is, the number of observations we have up to a certain time. Mendecki (2016) discusses the validity of the estimator and the number of samples needed to achieve reliable estimates of the upper limit, suggesting that at least seven record-breaking events are needed to provide a good estimate (see chapter 3.4.1 of Mendecki, 2016, for more details).

APPLICATION TO THREE TYPES OF INJECTION OR PRODUCTION ACTIVITIES

We applied the described methodology to catalogues of seismic events induced by reservoir production, hydraulic stimulation and saltwater disposal. The main goal of this application is to test the reliability of the methodology for predicting the maximum magnitude of the next breaking event. Therefore, we sought large catalogues ideally spanning many orders of magnitude to have as many record-breaking events as possible.

We start with a catalogue of induced seismicity resulting from gas production in the Groningen field, in the Netherlands (Bourne et al., 2014). We use a newly reassessed catalogue of events (Willacy et al., 2019) containing 1475 events recorded over 31 years of monitoring and production up to January 2022 (Oates et al., 2022). The catalogue contains all the large events from December 1991. The strongest, with M_L 3.6, occurred in August 2012. The local seismic monitoring network has been improving over time, particularly in the early 1990s and after 2011, resulting in the detection of weaker events with time. Hence, the completeness of the catalogue evolved, being greater than M_L 2.5 before 1995 (KNMI, 2022) and greater than M_L 1.5 since 1995 (Bourne et al., 2014).

Note that the low completeness before 1991 results in the first recorded record-breaking event of 2.4, which means a rise of 1.2 in magnitude between 1991 and 2012.

Figure 1 shows the time evolution of observed magnitudes in the Groningen field for events with $M_L > 0.9$. We can start to predict UL magnitudes from the July 1994 M_L 2.7 record-breaking event. The UL exactly predicts the magnitude of the next record-breaking event (NBRE) M_L 3.0 of October 2003 but underpredicts by 0.2 the August 2006 M_L 3.5 event. Prior to the largest event in 2012 (M_L 3.6), the UL forecast was M_L 4.0 and provides the current UL for the NBRE at M_L 4.2. This seems to be a very reasonable prediction within the lower bounds of the hazard assessment (NAM, 2022). The underprediction of the 2006 event probably results from the small number of record-breaking events up to that time and/or increased subsidence rates changing the statistical distribution of events at that period. We cannot exclude also some influence of magnitude calculation changing with the installation of greater numbers of stations. Nevertheless, the difference does not seem too large considering the uncertainty of the magnitude (at least 0.1). Unfortunately, the magnitude of completeness for events before 1991 limits the applicability of the method, it would be greatly beneficial to have a more complete dataset with historical detections as it is very unlikely that the seismicity in the Groningen field started with an M_L 2.4 event.

The next application of the methodology is shown in Figure 2 for the Quifa oil field in Colombia (Molina et al., 2020). We used the catalogue of the Colombian Geological Service (SGC) and tried to separate seismicity associated with the Quifa and Rubiales fields, according to the spatial location of the events. The catalogue spans 8 years starting in 2013 although injection precedes this date (Molina et al., 2020). The nearest SGC station was 40 km away limiting the threshold detection prior to 2014. After 2014, the seismic events in the area were detected by both local and national networks. Therefore, we show only events greater than M_L 2.5. We estimate the magnitude of completeness in the catalogue and area at M_L 2.5 (based on the Gutenberg–Richter magnitude frequency distribution). The largest event, recorded in March 2021, had a magnitude of M_L 5.0. Using the two record-breaking events in 2013, with a magnitude higher than 3.5, we can correctly predict the UL of all later events except M_L 4.3 in March 2014, although that is within the magnitude uncertainty.

The third application of the UL estimate is for hydraulic fracturing-induced seismicity at the Preston New Road wells in northern England in 2018–2019. We applied the methodology to combine catalogues of this induced seismicity from the North Sea Transition Authority with corrected magnitudes from the borehole and surface stations (Baptie et al., 2020; Kettley et al., 2021). The magnitudes of induced events from the North Sea Transition Authority had to be recalibrated to produce consistent magnitude estimates between surface and

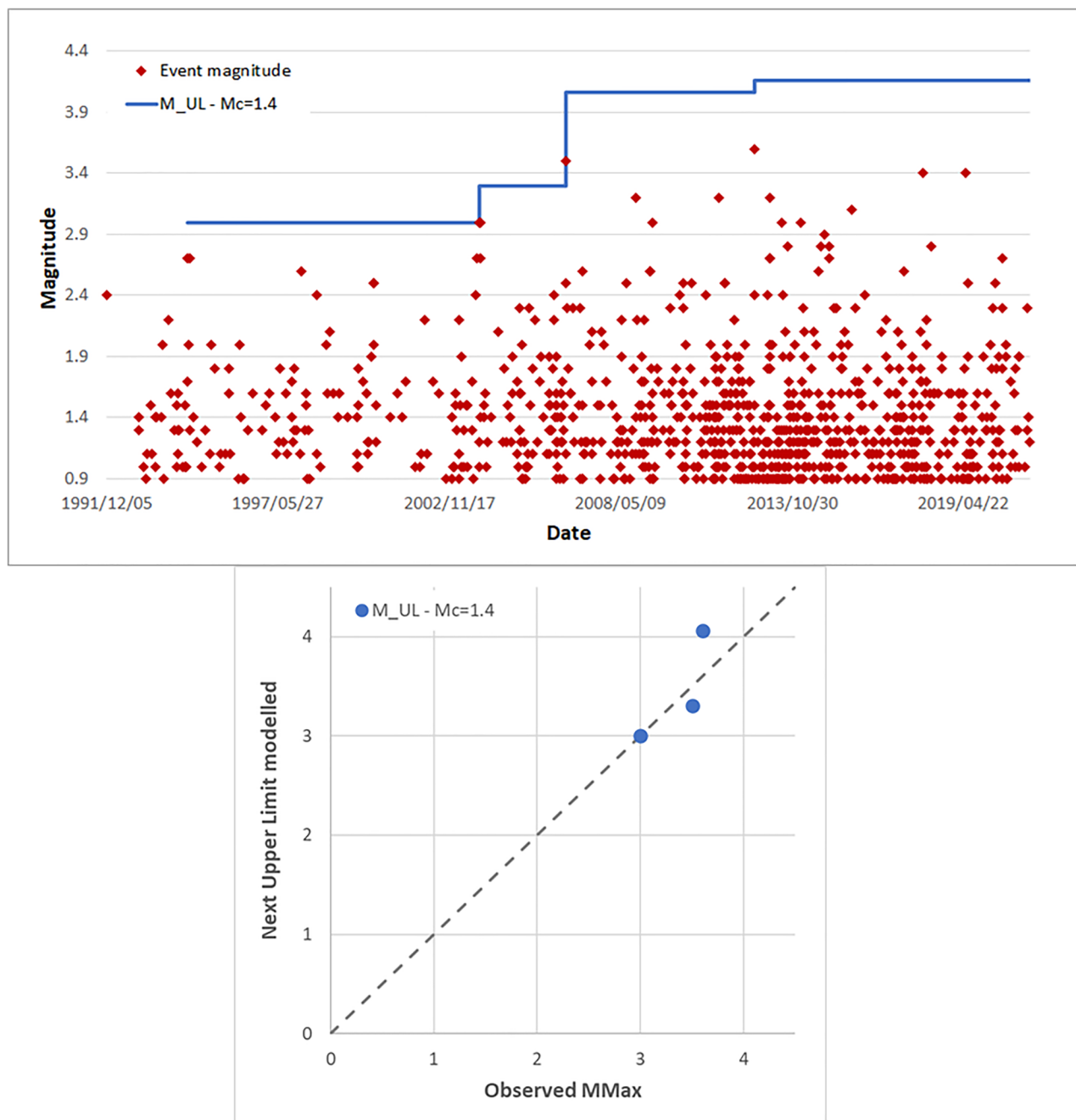


FIGURE 1 Top panel: Magnitude history (red dots) and upper limit magnitude prediction (blue line) for the Groningen gas field (Willacy et al., 2019). Bottom panel: Comparison between observed record-breaking and computed upper limit magnitudes.

downhole arrays as well as between the 2018 and 2019 stimulations (note that the positions of the surface and borehole monitoring networks were changed between 2018 and 2019; Kettlety et al., 2021).

Figure 3 shows different tests considering the injections in 2018 and 2019 as one or two independent injections. The high sensitivity of the network enables a low magnitude of completeness. This completeness of combined catalogues from 2018 to 2019 is at least -1.2 based on statistical analysis and lack of events with $M_w < -1.2$ in October 2018.

These resulted in 16 record-breaking events for the first stimulation (October to December 2018) and again 16 record-breaking events for the second stimulation (2019). Combining the catalogues from both stimulations (2018–2019) gives 19 record-breaking events, that is, 16 record-breaking events from 2018 and 3 record-breaking events from 2019.

The observed record-breaking magnitudes from induced seismicity of the stimulation in 2018 match the UL estimate almost perfectly, the UL mostly exceeds the observation by at most 0.2. The August–September 2019 stimulation UL values

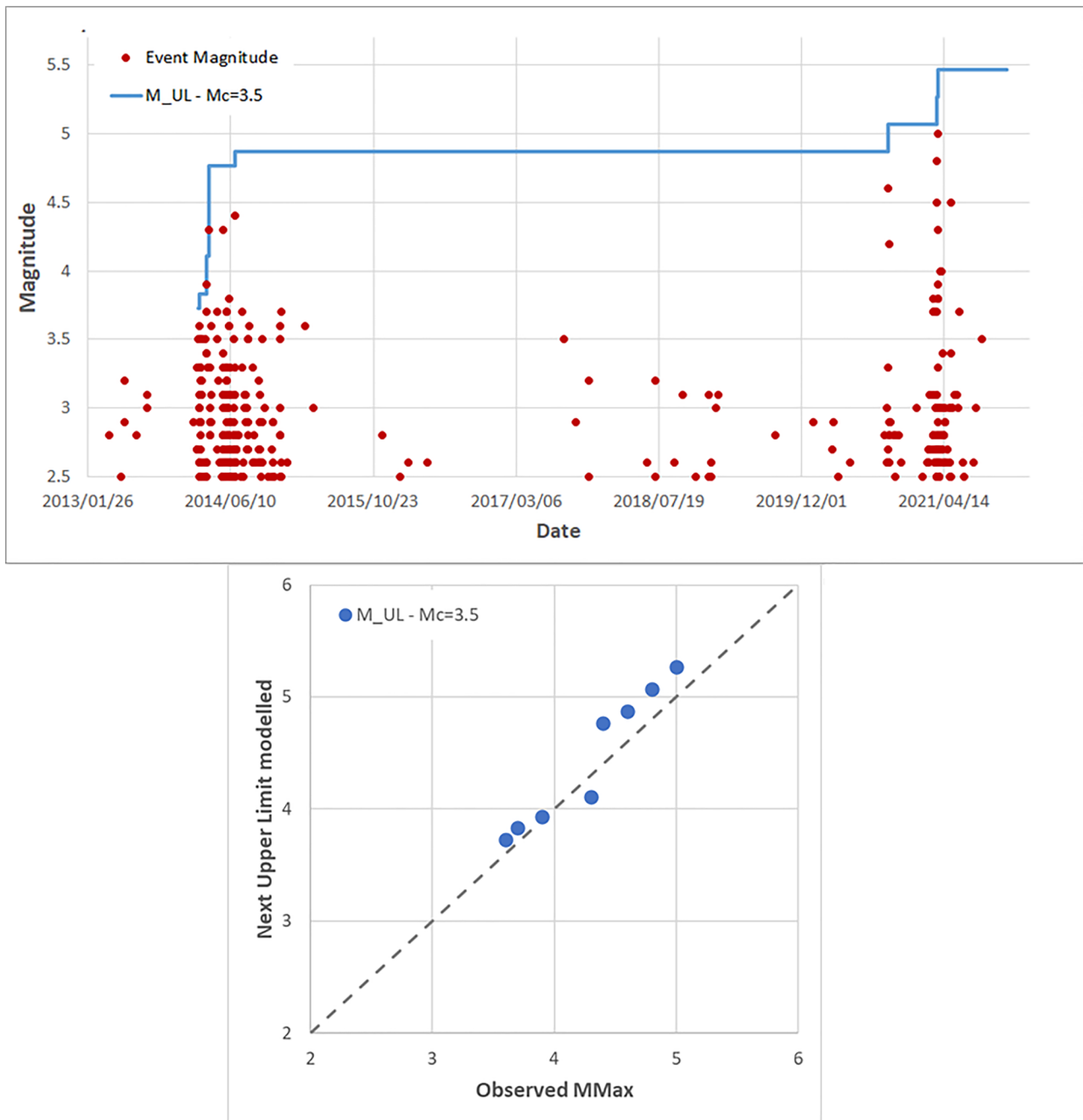


FIGURE 2 Top panel: Magnitude history (red dots) and upper limit magnitude prediction (blue line) for the Quifa oil field (Molina et al., 2020). Bottom panel: Comparison between observed record-breaking and computed upper limit magnitudes.

overestimate the observed record-breaking magnitudes by 0.3–0.4 for the first 13 events. However, the 14th event with M_w 1.94 is underestimated by 0.6, and the largest events of 2019, with magnitudes M_w 2.3 and M_w 2.8 are overestimated by 1.0 and 0.8, respectively. This considerably worse performance of the UL estimates for the 2019 catalogue may possibly result from the fact that the 2018 stimulation influenced the 2019 induced seismicity. Considering both catalogues together for 2018–2019, the UL overestimates the M_w 1.94 event but it bounds perfectly the event of M_w 2.3

and underestimates the event of M_w 2.8 by less than 0.2. These tests are consistent with the potential influence of the October–December 2018 hydraulic fracturing on the induced seismicity in 2019. However, this observation is only indirect evidence of such a long-term effect.

Finally, we use the datasets of Verdon and Bommer (2021), which represent publicly available hydraulic fracturing-induced seismicity datasets from a variety of regions. Figure 4 summarizes results for 15 datasets (including the three datasets discussed in detail above). Most of the observed

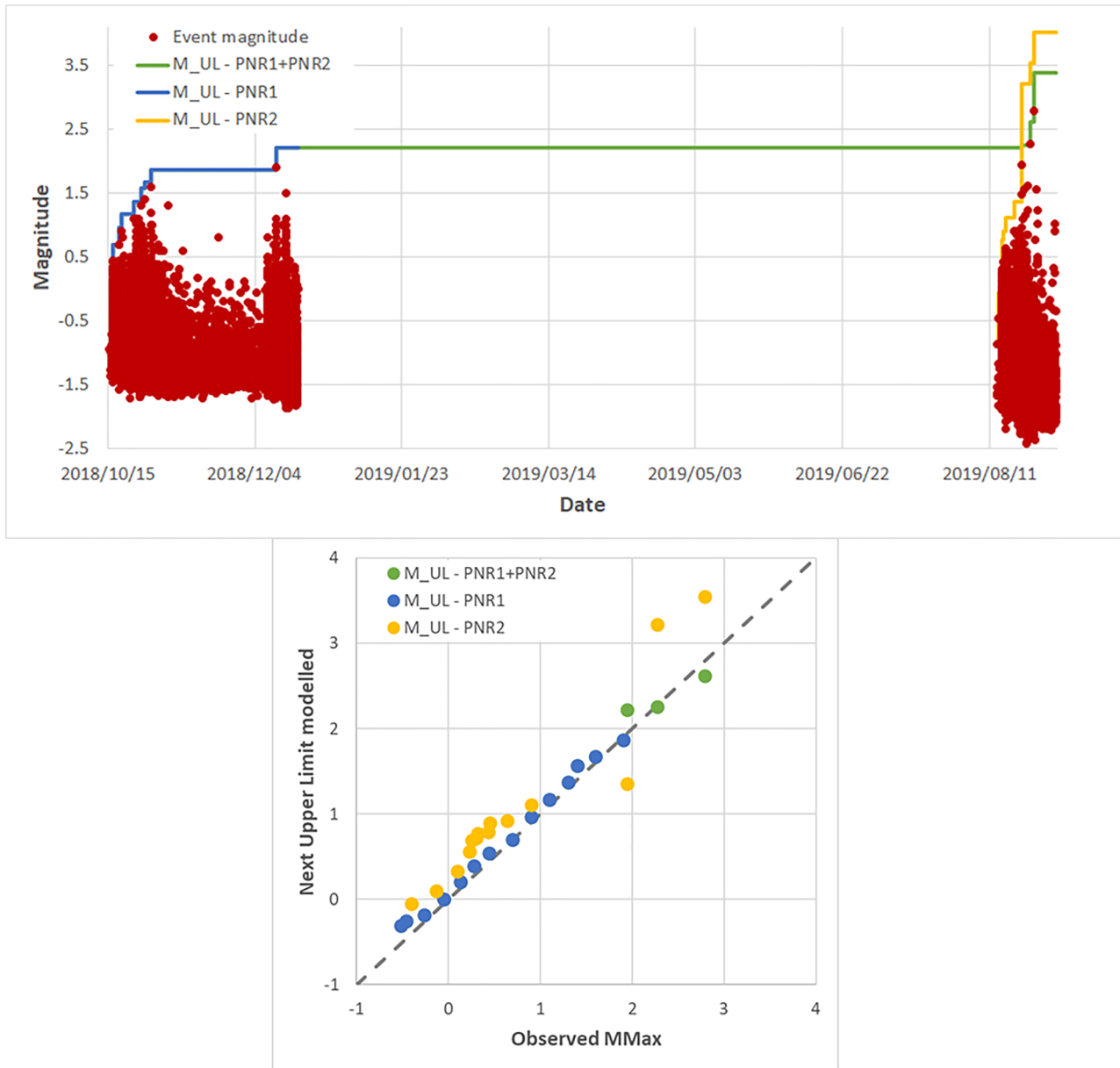


FIGURE 3 Top panel: Magnitude history (red dots) and upper limit magnitude prediction for induced seismicity by the Preston New Road hydraulic fracturing, for the first, the second and the first and second stimulations (blue, yellow and green lines). The magnitudes, from the North Sea Transition Authority catalogues, are obtained from corrected values from the borehole and surface stations. Bottom panel: Comparison between observed record-breaking and computed upper limit magnitudes.

record-breaking magnitudes are under the UL limit estimate or only slightly exceed it. For example, all observed events from the Bao and Eaton (2016) cases (C1–C6) are bound by the UL except six events, but these events exceed the prediction only by 0.25 at most. The longest record-breaking series of observed magnitudes is 19 events of the Tony Creek case (Eaton et al., 2018) (in the Duverney) where 18 magnitudes are correctly bound by the UL, then one event with record-breaking magnitude change from 1.5 to 2.4 was not forecast as the previous record-breaking changes were all smaller than 0.2 in that dataset. Similarly, the UL estimate

fails to bound the magnitude 3.1 event (which followed an M 1.4 event) in the Karnes (Eagle Ford) sequence (Fasola et al., 2019) by 1.1 magnitude units, and the magnitude 4.2 event (which followed an M 1.7 event) in the Red Deer ESB10 case (Schultz & Wang, 2020). We surmise that these failures are most likely related to situations where the nature of the induced seismicity has changed rapidly (for instance, a new fault has begun to reactivate as the area affected by stimulation increases), meaning that the foregoing seismicity no longer provides a useful forecast of upcoming events. However, through the majority of cases, as illustrated in Figure 4,

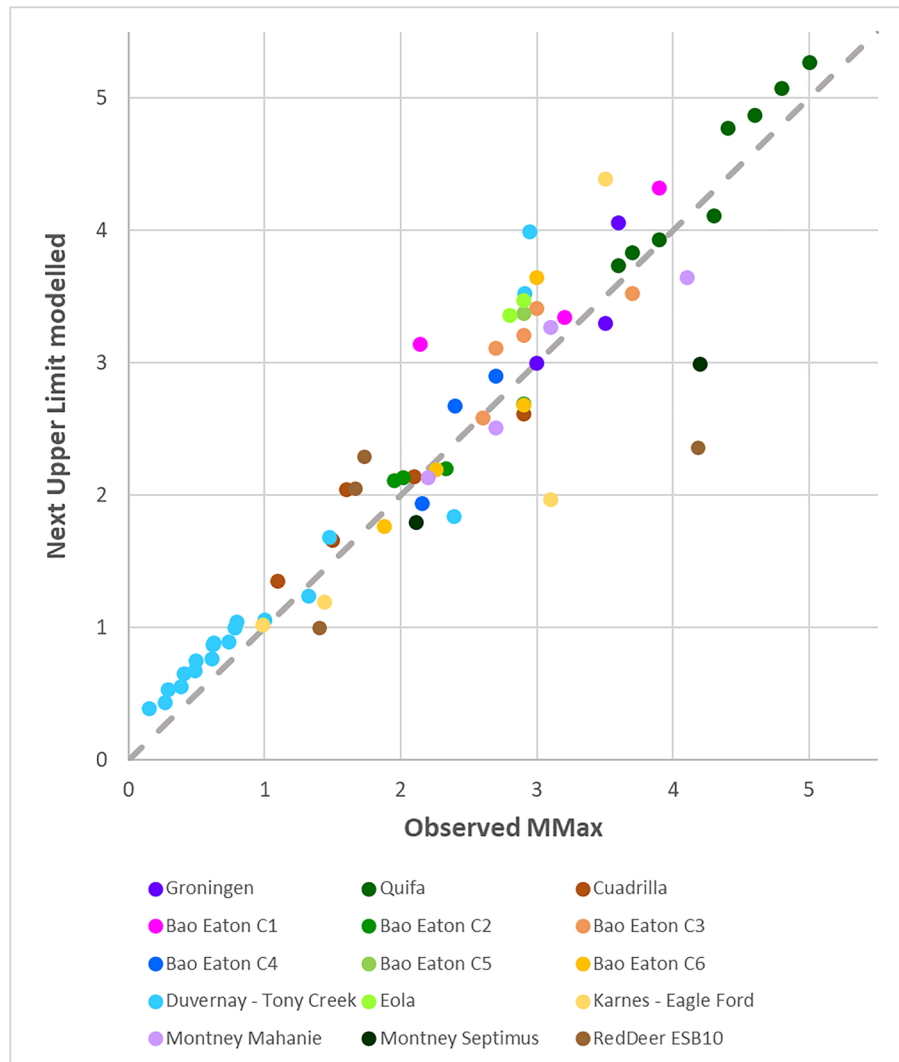


FIGURE 4 Comparison between observed record-breaking and the upper limit magnitude estimate.

the UL provides an upper bound to the next record-breaking events and the bound does not generally overestimate the next record-breaking event (mostly by less than 0.2).

DISCUSSION AND CONCLUSIONS

The methodology of the upper limit of the next record-breaking magnitude is not dependent on information like rate and volume of injection, size and orientation of faults, stress state and other parameters assuming some physical model. This is both an advantage and a disadvantage. We would prefer a deterministic model, but in the absence of a deterministic model we propose to use a statistical one. The statistics of record-breaking events reflect the physical processes – in an area where a small perturbation caused significant induced seismicity, the increases of the magnitudes will be large and the upper limit estimate will be large (see, for instance, Eisner et al., 2023). On the contrary, in a stable system where

significant perturbation is required to induce seismicity, the increases in magnitudes of record-breaking events will be small and the UL estimate will be only slightly larger than the previously observed record-breaking event.

A drawback of the methodology is the requirement of as complete as possible recording of the induced seismicity catalogue (as is the case for any method which uses observations of ongoing induced seismicity to forecast upcoming magnitudes). Our application to case studies indicates that even as little as two record-breaking events provide a reasonable upper limit estimate, but we should seek to observe at least five record-breaking events before predicting the upper limit. We generalize that the UL estimate does not bound the NBRE in exceptionally large steps in record-breaking magnitudes, especially if prior record-breaking events are increasing incrementally. The application to the large number of datasets shown in Figure 4 illustrates that the UL underestimation by more than 0.5 occurs mostly when less than five record-breaking events are available (except for the Tony Creek

dataset). This implies the need to have a monitoring network capable of recording at least five record-breaking events before the magnitude of concern. This means the seismic-monitoring network must be able to detect seismic events at least 1.5, but preferably 2.0 magnitude units lower than the magnitude we want to be able to forecast, which is consistent with conclusions of Verdon and Bommer (2021).

Varty et al. (2021) raised the issue of rounding statistical variables – such as magnitudes – to the first decimal point, resulting in statistical bias. This is of particular concern in this proposed methodology as we use differences in the rounded magnitudes. We have carried out tests (Mendecki, 2023) with magnitudes rounded to the first and second decimals place and obtained similar results for UL bounds. We believe this can be explained by the fact that in Equation (2) the largest differences in observed record-breaking magnitudes have the largest influence on the UL estimate. Larger differences in magnitudes will be less affected by rounding and therefore, the UL estimate is relatively unaffected.

We observed issues with self-inconsistency of magnitude determination for a number of datasets. The magnitudes must be self-consistent; otherwise, we are not observing the distribution of natural events but errors, and such data will not provide useful predictions. This is a sensitive issue for induced seismicity monitoring where the combined use of data recorded on downhole, local temporary surface monitoring and regional networks may result in greater inconsistencies (Kendall et al., 2019; Kettlety et al., 2021; Viegas et al., 2012) when compared to permanent surface networks used for natural seismicity. The UL estimates provide a scientific estimate of what can be expected if the energy operations continue as they were up to the chosen time. If such an estimate exceeds a set threshold, changes in energy extractions can be taken to alter the distribution of induced events.

ACKNOWLEDGEMENTS


The authors are grateful for the great help of Alexander Mendecki while developing and applying this methodology. The authors also benefited from the great discussion during the Mmax workshop organized by NAM. We acknowledge the generous support by the College of Petroleum Engineering and Geosciences (CPG) at King Fahd University of Petroleum and Minerals (KFUPM) through grant no. CPG-21103.


DATA AVAILABILITY STATEMENT


The data that support the findings of this study were derived from the following resources available in the public domain: Willacy et al. (2019), <https://www.sgc.gov.co/sismos> and Verdon and Bommer (2021).

ORCID

Leo Eisner  <https://orcid.org/0000-0001-6376-4014>

Zuzana Jechumtálová  <https://orcid.org/0000-0001-5881-1234>

James Verdon  <https://orcid.org/0000-0002-8410-2703>

Umair Bin Waheed  <https://orcid.org/0000-0002-5189-0694>

REFERENCES

- Bao, X. & Eaton, D.W. (2016) Fault activation by hydraulic fracturing in western Canada. *Science*, 354, 1406–1409.
- Baptie, B., Luckett, R., Butcher, A. & Werner, M. (2020) Robust relationships for magnitude conversion of PNR seismicity catalogues. British Geological Survey Open Report, OR/20/042.
- Barlow, A.M., Sherlock, C. & Tawn, J. (2020) Inference for extreme values under threshold-based stopping rules. *Journal of the Royal Statistical Society: Series C (Applied Statistics)*, 69(4), 765–789.
- Bommer, J., Oates, S., Cepeda, J.M., Lindholm, C., Bird, J., Torres, R., Marroquín, G. & Rivas, J. (2006) Control of hazard due to seismicity induced by a hot fractured rock geothermal project. *Engineering Geology*, 83(4), 287–306.
- Bourne, S., Oates, S., van Elk, J.F. & Doornhof, D. (2014) A seismological model for earthquakes induced by fluid extraction from a subsurface reservoir. *Journal of Geophysical Research: Solid Earth*, 119(12), 8991–9015.
- Cao, N.-T., Eisner, L. & Jechumtálová, Z. (2020) Next record-breaking magnitude for injection induced seismicity. *First Break*, 38(2), 53–57.
- Clarke, H., Verdon, J., Kettlety, T., Baird, A. & Kendall, M. (2019) Real-time imaging, forecasting, and management of human-induced seismicity at Preston New Road, Lancashire, England. *Seismological Research Letters*, 90(5), 1902–1915.
- Cooke, P.J. (1979) Statistical inference for bounds of random variables. *Biometrika*, 66(2), 367–374.
- Dahm, T., Cesca, S., Hainzl, S., Braun, T. & Krüger, F. (2015) Discrimination between induced, triggered, and natural earthquakes close to hydrocarbon reservoirs: a probabilistic approach based on the modeling of depletion-induced stress changes and seismological source parameters. *Journal of Geophysical Research: Solid Earth*, 120(4), 2491–2509.
- Eaton, D.W., Igonin, N., Poulin, A., Weir, R., Zhang, H., Pellegrino, S. & Rodriguez, G. (2018) Induced seismicity characterization during hydraulic-fracture monitoring with a shallow-wellbore geophone array and broadband sensors. *Seismological Research Letters*, 89(5), 1641–1651.
- Eisner, L., Cao, N.-T., Verdon, J.P., Jechumtálová, Z., bin Waheed, U. & Stanek, F. (2023) Evaluating monitoring array performance using upper limit magnitude prediction. In *84th EAGE Annual Conference & Exhibition*, volume 2023. Houten, the Netherlands: European Association of Geoscientists & Engineers, pp. 1–5.
- Fasola, S., Brudzinski, M.R., Skoumal, R.J., Langenkamp, T., Currie, B.S., & Smart, K.J. (2019) Hydraulic fracture injection strategy influences the probability of earthquakes in the Eagle Ford Shale play of South Texas. *Geophysical Research Letters*, 46, 12958–12967.
- Halló, M., Opršal, I., Eisner, L. & Ali, M.Y. (2014) Prediction of magnitude of the largest potentially induced seismic event. *Journal of Seismology*, 18(3), 421–431.
- Healy, J.H., Rubey, W.W., Griggs, D.T. & Raleigh, C.B. (1968) The Denver earthquakes. *Science*, 161(3848), 1301–1310.
- Kendall, J., Butcher, A., Stork, A.L., Verdon, J.P., Luckett, R. & Baptie, B.J. (2019) How big is a small earthquake? Challenges in determining microseismic magnitudes. *First Break*, 37(2), 51–56.
- Kettlety, T., Verdon, J., Butcher, A., Hampson, M. & Craddock, L. (2021) High-resolution imaging of the ML 2.9 August 2019 earthquake in Lancashire, United Kingdom, induced by hydraulic fracturing

- during Preston New Road PNR-2 operations. *Seismological Research Letters*, 92(1), 151–169.
- Kettlety, T., Verdon, J., Werner, M. & Kendall, M. (2020) Stress transfer from opening hydraulic fractures controls the distribution of induced seismicity. *Journal of Geophysical Research: Solid Earth*, 125(1), e2019JB018794.
- Kijko, A. (2004) Estimation of the maximum earthquake magnitude, m_{max} . *Pure and Applied Geophysics*, 161, 1655–1681.
- Kivi, I.R., Pujades, E., Rutqvist, J. & Vilarrasa, V. (2022) Cooling-induced reactivation of distant faults during long-term geothermal energy production in hot sedimentary aquifers. *Scientific Reports*, 12(1), 2065.
- Kwiatek, G., Saarno, T., Ader, T., Blümle, F., Bohnhoff, M., Chendorain, M., Dresen, G., Heikkinen, P., Kukkonen, I., Leary, P., Leonhardt, M., Malin, P., Martínez-Garzón, P., Passmore, K., Passmore, P., Valenzuela, S. & Wollin, C. (2019) Controlling fluid-induced seismicity during a 6.1-km-deep geothermal stimulation in Finland. *Science Advances*, 5(5), eaav7224.
- Mancini, S., Werner, M., Segou, M. & Baptie, B. (2021) Probabilistic forecasting of hydraulic fracturing induced seismicity using an injection-rate driven ETAS model. *Seismological Research Letters*, 92(6), 3471–3481.
- Mendecki, A.J. (2012) Size distribution of seismic events in mines. In *Proceedings of the Australian Earthquake Engineering Society 2012 Conference*, 7–9 December 2012, Queensland, Australia. Richmond, Australia, Australian Earthquake Engineering Society, pp. 1–20.
- Mendecki, A.J. (2013) Characteristics of seismic hazard in mines. In *Proceedings 8th International Symposium on Rockbursts and Seismicity in Mines*, Russia, 2013. Obninsk, Russia: Geophysical Survey of Russia Academy of Sciences, pp. 275–292.
- Mendecki, A.J. (2016) *Mine seismology reference book: Seismic hazard*. Kingston, Australia: Institute of Mine Seismology.
- Molina, I., Velasquez, J.S., Rubinstein, J., Garcia, A. & Dionicio, V. (2020) Seismicity induced by massive wastewater injection near Puerto Gaitán, Colombia. *Geophysical Journal International*, 223(2), 777–791.
- NAM. (2022) Report on the Second Workshop on Mmax for seismic hazard and risk analysis in the Groningen Gas Field. Assen, Netherlands: Nederlandse Aardolie Maatschappij B.V.
- Nantanoi, S., Rodríguez-Pradilla, G. & Verdon, J.P. (2022) 3D seismic interpretation and fault slip potential analysis from hydraulic fracturing in the Bowland Shale, UK. *Petroleum Geology*, 28(2), petgeo2021–057.
- Oates, S., Landman, A.J., van der Wal, O., Baehr, H. & Piening, H. (2022) Geomechanical, seismological, and geodetic data pertaining to the Groningen gas field: a data package used in the ‘Mmax II Workshop’, on constraining the maximum earthquake magnitude in the Groningen field. <https://public.yoda.uu.nl/geo/UU01/RHHRPY.html>
- Palgunadi, K.H., Gabriel, A.-A., Ulrich, T., Ángel López-Comino, J. & Mai, P.M. (2020) Dynamic fault interaction during a fluid-injection induced earthquake: The 2017 Mw 5.5 Pohang event. *Bulletin of the Seismological Society of America*, 110(5), 2328–2349.
- Schultz, R., Beroza, G.C. & Ellsworth, W.L. (2021) A strategy for choosing red-light thresholds to manage hydraulic fracturing induced seismicity in North America. *Journal of Geophysical Research: Solid Earth*, 126(12), e2021JB022340.
- Schultz, R. & Wang, R. (2020) Newly emerging cases of hydraulic fracturing induced seismicity in the Duvernay East Shale Basin. *Tectonophysics*, 779, 228393.
- Segall, P. (1989) Earthquakes triggered by fluid extraction. *Geology*, 17(10), 942–946.
- Shapiro, S., Dinske, C., Langenbruch, C. & Wenzel, F. (2010) Seismological index and magnitude probability of earthquakes induced during reservoir fluid stimulations. *The Leading Edge*, 29(3), 304–309.
- Spearing, H., Tawn, J., Irons, D., Paulden, T. & Bennett, G. (2020) Ranking, and other properties, of elite swimmers using extreme value theory. *Journal of the Royal Statistical Society: Series A (Statistics in Society)*, 184(4), 368–395.
- Tata, M.N. (1969) On outstanding values in a sequence of random variables. *Zeitschrift für Wahrscheinlichkeitstheorie und Verwandte Gebiete*, 12(1), 9–20.
- Van Aalsburg, J., Newman, W.I., Turcotte, D.L. & Rundle, J.B. (2010) Record-breaking earthquakes. *Bulletin of the Seismological Society of America*, 100(4), 1800–1805.
- van der Elst, N.J., Page, M.T., Weiser, D.A., Goebel, T. H.W. & Hosseini, S.M. (2016) Induced earthquake magnitudes are as large as (statistically) expected. *Journal of Geophysical Research*, 121, 4575–4590.
- Varty, Z., Tawn, J.A., Atkinson, P.M. & Bierman, S. (2021) Inference for extreme earthquake magnitudes accounting for a time-varying measurement process. <https://doi.org/10.48550/arXiv.2102.00884>
- Verdon, J. & Bommer, J. (2021) Green, yellow, red, or out of the blue? An assessment of Traffic Light Schemes to mitigate the impact of hydraulic fracturing-induced seismicity. *Journal of Seismology*, 25(1), 301–326.
- Verdon, J., Stork, A., Bissell, R., Bond, C. & Werner, M. (2015) Simulation of seismic events induced by CO₂ injection at In Salah, Algeria. *Earth and Planetary Science Letters*, 426, 118–129.
- Viegas, G., Baig, A., Coulter, W. & Urbancic, T. (2012) Effective monitoring of reservoir-induced seismicity utilizing integrated surface and downhole seismic networks. *First Break*, 30(7), 77–81.
- Vlek, C. (2019) The Groningen gasquakes: Foreseeable surprises, complications of hard science, and the search for effective risk communication. *Seismological Research Letters*, 90(3), 1071–1077.
- Willacy, C., van Dedem, E., Minisini, S., Li, J., Blokland, J.-W., Das, I. & Droujinine, A. (2019) Full-waveform event location and moment tensor inversion for induced seismicity. *Geophysics*, 84(2), KS39–KS57.
- Yoder, M., Turcotte, D. & Rundle, J. (2010) Record-breaking earthquake intervals in a global catalogue and an aftershock sequence. *Nonlinear Processes in Geophysics*, 17, 169–176.
- Zoback, M.D. (2007) *Reservoir geomechanics*. Cambridge, UK: Cambridge University Press.

How to cite this article: Cao, N.-T., Eisner, L., Jechumtálová, Z., Verdon, J. & Waheed, U.B. (2024) Upper limit magnitudes for induced seismicity in energy industries. *Geophysical Prospecting*, 1–10. <https://doi.org/10.1111/1365-2478.13553>